Phase Identification of Cu-In Alloys with 45 and 41.25 at.% In Compositions

L. Baqué, D. Torrado, G. Aurelio, D. G. Lamas, S. F. Aricó, A. F. Craievich & S. Sommadossi

Journal of Phase Equilibria and Diffusion

ISSN 1547-7037

J. Phase Equilib. Diffus.
DOI 10.1007/s11669-013-0265-7

Springer

JPEDAV
DOI: 10.1007/s11669-013-0265-7
1547-7037 ©ASM International

Phase Identification of Cu-In Alloys with 45 and 41.25 at.% In Compositions

L. Baqué, D. Torrado, G. Aurelio, D.G. Lamas, S.F. Aricó, A.F. Craievich, and S. Sommadossi

(Submitted April 22, 2013; in revised form July 6, 2013)

In this work, the thermal stability of Cu-In alloys with 45.0 and 41.2 at.% In nominal compositions was investigated by differential scanning calorimetry (DSC), scanning electron microscopy, wavelength dispersive spectroscopy, and in-situ synchrotron x-ray powder diffraction (S-PXRD) over a temperature range from 25 up to 400 °C. The studied samples are mainly composed of a $Cu_{11}In_9$ phase together with minor amounts of the B phase (based on the NiAs-Ni_2In type structure) and, in one of the samples, with a minor amount of pure In. No evidence of the $Cu_{10}In_7$ (41.2 at.% In) phase was detected, not even in the sample with 41.2 at.% In nominal overall composition. The combined use of the S-PXRD and DSC techniques allowed us to identify two phase transitions involving the $Cu_{11}In_9$ phase, one of them corresponding to the $\eta' \rightleftharpoons B + Cu_{11}In_9$ reaction at $T = 290$ °C and the other to the peritectic $\eta' + L \rightleftharpoons Cu_{11}In_9$ reaction at $T = 311$ °C.

Keywords Cu-In alloys, differential scanning calorimetry (DSC), intermetallic compounds, phase transitions

1. Introduction

The Cu-In-Sn ternary system is a Pb-free environment-friendly alternative for replacing conventional Pb-based solders in the electronic industry.[1-3] Therefore, many investigations were conducted in order to study the fundamental properties of Cu-In-Sn materials and to predict their practical behavior.[2,3] The formation of binary phases capable of incorporating small quantities of a third element in their crystal structure such as $Cu_{11}(In,Sn)_9$, η-$Cu_2(In,Sn)$ and δ-$Cu_7(In,Sn)_3$, η-$Cu_6(Sn,In)_5$, and ζ-$Cu_{10}(Sn,In)_3$ were observed in Cu/In-Sn/Cu joints.[4-6] However, discrepancies still remain not only concerning the Cu-In-Sn ternary phase diagram but also the Cu-In, Cu-Sn, and In-Sn binary diagrams.[2]

One of the most controversial fields of the Cu-In binary phase diagram lies between ~33 and 38 at.% In and between temperatures from 100 up to 500 °C. According to different authors, at high temperature (above ~350 °C), this system exhibits either three phases A, A′ and H as shown in Fig. 1(a),[7,8] or only one phase, namely phase η′ as can be seen in Fig. 1(b).[9,10] On the other hand, at low temperature, some authors proposed the existence of two phases, B and C as shown in Fig. 1(a)[7,8] and others the presence of only the phase η as can be seen in Fig. 1(b).[9,10] Even more, Elding-Pontén et al.[11] have shown by electron diffraction patterns that the η field is a multi-phase region containing a continuous range of modulated structures which can be classified in three distinct phase regions, namely A, B and C.

We have recently reported the presence of phase A in samples with 32-37 at.% In nominal composition annealed during 7 months at 500 °C.[12] We have also observed the presence of phase B in a Cu-37 at.% In alloy and phase C in alloys containing 32 and 34 at.% In, all of them after being annealed during 7 months at 300 °C. In terms of their crystallography, phases A, B, and C present NiAs-Ni_2In-type structures[11,12] and can be described as superstructures of the Cu_2In phase.[13] By comparing Fig. 1(a) and (b), we can realize that these phase diagrams show clear differences not only in the 32-37 at.% In range but also in the range from 37 at.% In up to 45 at.% In.

More recently, Piao and Lidin[14] reported the presence of a novel phase, $Cu_{10}In_7$, in a Cu-In alloy with 41.2 at.% In after a long heat treatment of 9 months at 310 °C. The authors claim that a very long annealing promotes the transformation from a disordered $Cu_{11}In_9$ phase to a denser and ordered $Cu_{10}In_7$ compound, and that this would also explain why the presence of this compound had not been reported previously. A further finding of a metastable CuIn stoichiometric phase in Cu-50 at.% In samples was also reported.[15,16]

L. Baqué, Department of Energy Conversion and Storage, Technical University of Denmark, Frederiksborgvej 399, 4000 Roskilde, Denmark; and CCT-Comahue, CONICET, Buenos Aires 1400, 8300 Neuquén, Argentina; **D. Torrado,** Engineering Faculty, Comahue National University, Buenos Aires 1400, 8300 Neuquén, Argentina; **G. Aurelio,** CONICET/Centro Atómico Bariloche, Av. Bustillo 9500, 8400 San Carlos de Bariloche, Argentina; **D.G. Lamas,** Engineering Faculty, Comahue National University, Buenos Aires 1400, 8300 Neuquén, Argentina; and CCT-Comahue, CONICET, Buenos Aires 1400, 8300 Neuquén, Argentina; **S.F. Aricó,** Departamento de Materiales, CAC-CNEA, Av. Gral. Paz 1499, B1650KNA San Martín, Argentina; **A.F. Craievich,** Institute of Physics, University of São Paulo, Rua do Matao, Travessa R, 187, São Paulo CEP 05508-900, Brazil; and **S. Sommadossi,** Engineering Faculty, Comahue National University, Buenos Aires 1400, 8300 Neuquén, Argentina; and CCT-Comahue, CONICET, Buenos Aires 1400, 8300 Neuquén, Argentina. Contact e-mails: silvana.sommadossi@fain.uncoma.edu.ar, ssommadossi@gmail.com

Published online: 12 October 2013

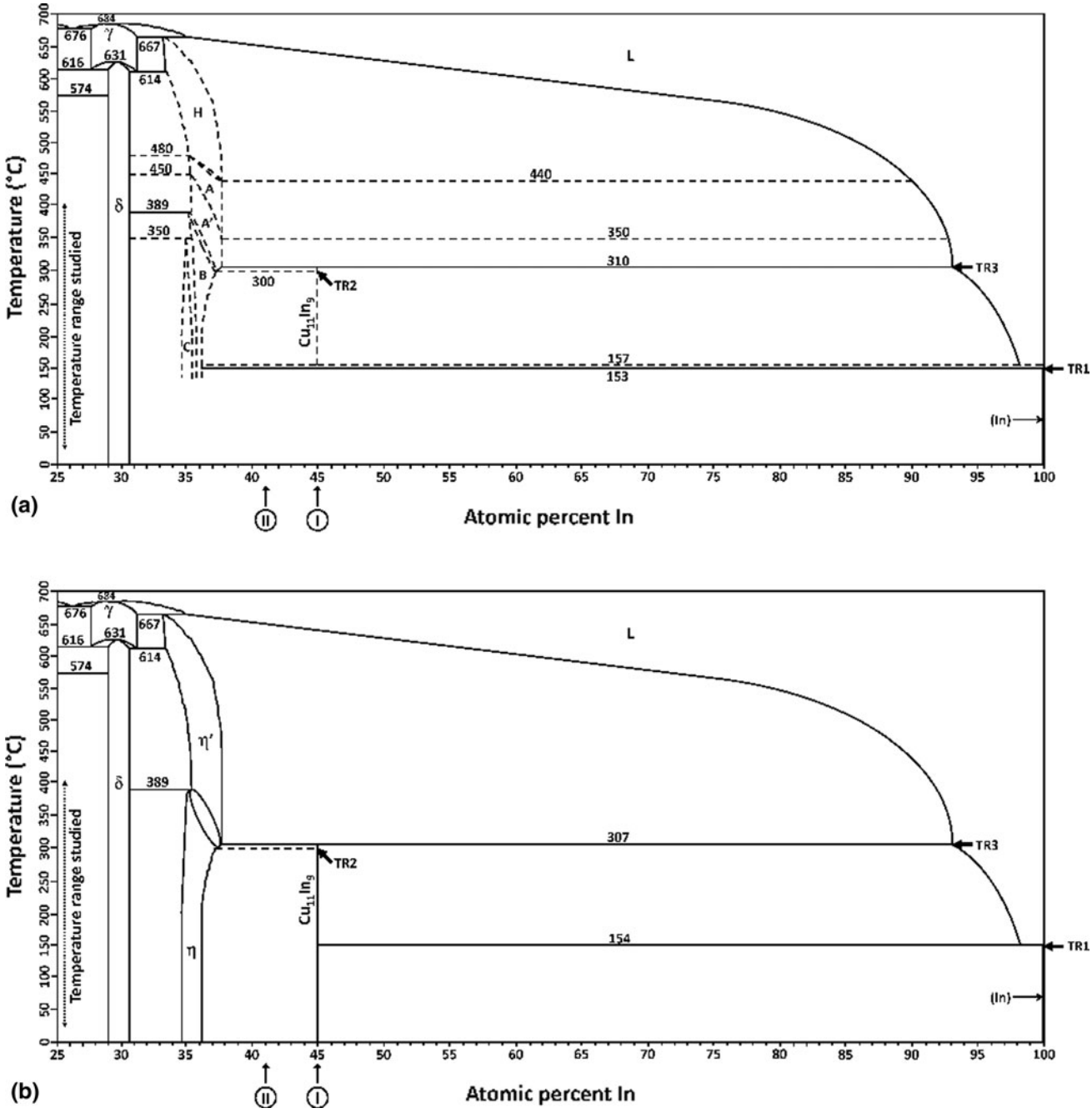

Fig. 1 Cu-In phase diagram according to (a) Subramanian and Laughlin[8] and (b) Bolcavage et al.[9] The composition of samples studied in this work (named I and II) and the observed transformations (TR) are indicated

The thermodynamic stability of the $Cu_{11}In_9$ phase is also under discussion. As a matter of fact, Subramanian and Laughlin[8] suggested that the decomposition of the $Cu_{11}In_9$ phase occurs at 157 °C via a metatectic reaction (Fig. 1a) while others[9,10] indicated the existence of a $Cu_{11}In_9$ phase at room temperature without finding any evidence of the metatectic reaction (Fig. 1b).

There is now a general consensus about the fact that the $Cu_{11}In_9$ phase with a nominal composition of 45.0 at.% In is formed peritectically. However a discrepancy still remains regarding the precise temperature at which this reaction occurs, namely 310 and 307 °C as shown in Fig. 1(a) and (b), respectively.

The present work aims at studying the thermal stability of two binary Cu-In alloys, with 45 and 41.2 at.% In nominal compositions named as sample I and sample II, respectively, over the 25-400 °C temperature range. The combination of several characterization techniques, namely differential scanning calorimetry (DSC), synchrotron x-ray powder diffraction (S-PXRD), scanning electron microscopy (SEM), and

wavelength dispersive spectroscopy (WDS), is expected to elucidate the controversies mentioned above. The S-PXRD study reported here was performed in-situ using a high temperature chamber attached to a S-PXRD beam line. To the best of our knowledge, this is the first in-situ XPD study of phase transformations occurring in the Cu-In system.

2. Experimental

Two Cu-In alloys with 45.0 at.% In (sample I) and 41.2 at.% In (sample II) were prepared. Ten grams of sample were produced per each alloy. A 99.999% Cu ingot together with a 99.999% In ingot were melted in quartz ampoules (previous vacuum and refilled with Ar) using H_2 torch with agitation for 5 min to guarantee a good mixing in the molten metal. Then the ampoules were cooled down to room temperature in air. Additional care was taken for the alloy preparation in order to inhibit the In evaporation during casting and the mass was checked properly. Both samples were subsequently annealed in a resistive furnace under Ar atmosphere during 7 months at 300 °C and then quenched down to room temperature.

The microstructure of the samples was analyzed by using a Philips 515 SEM. Images were acquired using backscattered electrons in order to maximize atomic number contrast. The surface of the alloys for microscopic inspection was polished by using wet SiC papers down to 4000 grit and soft cloth with diamond paste down to 1 μm using distillated water and soap as lubricant.

Lineal composition profiles with 1 μm steps were obtained using the WDS technique employing a Cameca SX50 electron microprobe under an accelerating potential of 20 kV. This equipment was recalibrated before each analysis session using pure 99.999 wt.% Cu and 99.999 wt.% In standards.

The thermal stability of the samples was investigated by DSC analysis under N_2 flow using a TA Instruments 2910 calorimeter with a 2 °C/min heating rate. Aluminum pans and lids were used to encapsulate the alloys and empty holders were used as reference. The initial and maximum temperatures in each transition were determined using the TA Universal Analysis 2000 software. This software determines the integral of the DSC peaks assuming a linear background.

In order to investigate the thermal stability of the phases in the studied alloys, in-situ high temperature S-PXRD measurements were performed at the D10B-XPD beam line of the Brazilian Synchrotron Light Laboratory, LNLS, Campinas, Brazil. An x-ray beam with a wavelength $\lambda = 1.441$ Å under a high-intensity configuration, i.e., without crystal analyzer, was used to obtain optimal diffracted intensity. The S-PXRD measurements were performed using stainless steel sample holders with flat-plate shape in reflection geometry. X-ray diffraction patterns were recorded in-situ starting from 25 up to 400 °C, over the $27° \leq 2\Theta \leq 31°$ angular range. The minimum counting time was 0.7 s/step, and the heating rate equal to 2 °C/min. The powdered alloy was kept under Ar atmosphere during the high temperature S-PXRD measurements.

Additional S-PXRD patterns were recorded over a large angular range ($15° \leq 2\Theta \leq 85°$) at two (low and high) temperatures, namely 25 and 400 °C, which correspond to the initial and final temperatures of the heating ramp.

Fine powder samples suitable for S-PXRD were obtained by milling the alloys in an agate mortar and then sieving them through a 20 μm mesh. Nevertheless, the resulting crystallite sizes were not small enough to achieve sufficient randomness in the orientation of the crystallite sizes required to perform Rietveld refinements. However, the procedure used demonstrated to be adequate for the characterization of the thermal stability of the different detected phases thus allowing us to fulfill the objectives of this work.

Phase identification was performed by analyzing the position and intensity of all the peaks observed in each diffractogram. The crystal structure data of the relevant phases are summarized in Table 1. For the phases whose crystal structure was previously known (i.e. $Cu_{11}In_9$, η′, CuIn, $Cu_{10}In_7$, In, In_2O_3), the expected x-ray diffraction patterns were simulated using FullProf Suite software[21] using the wavelength of the experiment as well as the instrumental resolution function. The experimental patterns were compared with the simulated ones in order to identify the presence of minor phases. Moreover, we have carefully analyzed all experimental x-ray diffraction patterns paying especial attention to the eventual presence of low intensity peaks.

In order to detect the eventual presence of metastable phases developed during the homogenization annealing and/or during quenching, the DSC and S-PXRD measurements were performed during two successive heating/cooling cycles.

3. Results and Discussion

3.1 Characterization of the As-Quenched Samples

Three phases were identified in the SEM image displayed in Fig. 2(a) corresponding to sample I (45.0 at.% In). The compositions of these three phases were determined from the analysis of the WDS line scan shown in Fig. 2(b). Taking into account this result and the qualitative analysis of the morphology of SEM images, we conclude that the phase exhibiting the highest roughness in Fig. 2(a) is pure solidified In, this phase being retained after cooling from the high temperature In-rich liquid phase. The second phase with smoother morphology in Fig. 2(a) exhibits a Cu_2In composition. Between these two phases, the presence of faceted grains typical of the $Cu_{11}In_9$ phase[22] is apparent. The irregular structural features between $Cu_{11}In_9$ and pure In phases would explain the presence of a 10 μm thick smooth transition in composition observed in Fig. 2(b).

S-PXRD patterns corresponding to samples I and II, recorded at room temperature, are displayed in Fig. 3(a) over the 20-45° 2Θ range. A first qualitative analysis of both patterns indicates that most of the diffraction peaks correspond to the $Cu_{11}In_9$[17] and B phases.[11,12] A few very low intensity peaks in the diffraction patterns of samples I and II could not be identified.

Table 1 Literature crystal structure data used for identifying the phases present in the samples investigated in the present work

Name	Stoichiometry	Space group symbol	Pearson symbol	Lattice parameters	PDF/ICSD Card	References
$Cu_{11}In_9$	$Cu_{0.55}In_{0.45}$	*C*2/*m*	*mC*20	*a* = 12.814 Å *b* = 4.3543 Å *c* = 7.353 Å β = 54.59°	PDF 00-041-0883	17
η′ (or H)	$Cu_{0.66}In_{0.33}$	$P6_3/mmc$	*hP*6	*a* = 4.2943 Å *c* = 5.2328 Å	PDF 00-042-1475	7, 13
A	$Cu_{0.64}In_{0.36}$	Orthorhombic system	*oP*50	*a* = 21.375 Å *b* = 7.405 Å *c* = 5.218 Å	PDF 00-026-0523	7
A′	$Cu_{0.64}In_{0.36}$	Orthorhombic system	*oP*75	*a* = 34.194 Å *b* = 7.395 Å *c* = 5.262 Å	PDF 00-026-0522	7
A	33-40 at.% In	$P6_3/mmc$	*hP*600	*a* = 42.86 Å *c* = 5.263 Å	···	11, 12
B	34-37 at.% In	$P6_3/mmc$	*hP*600	*a* = 42.76 Å *c* = 5.278 Å	···	11, 12
C	$Cu_{0.66}In_{0.34}$	Orthorhombic system	No reported	*a* = 38.39 Å *b* = 7.388 Å *c* = 20.972 Å	···	11
CuIn	$Cu_{0.5}In_{0.5}$	$P2_1/m$	*mP*40	*a* = 7.191 Å *b* = 14.499 Å *c* = 10.28 Å β = 133.79°	PDF 00-035-1150	15
$Cu_{10}In_7$	$Cu_{0.588}In_{0.412}$	*C*2/*m*	*mS*68	*a* = 13.8453 Å *b* = 11.8462 Å *c* = 6.7388 Å β = 91.063°	ICSD #246130	14, 18
Indium	In	*I*4/*mmm*	*tI*2	*a* = 3.2517 Å *c* = 4.9459 Å	PDF 00-005-0642	19
Indium oxide	In_2O_3	*Ia*−3	*cI*80	*a* = 10.118 Å	PDF 00-006-0416	20

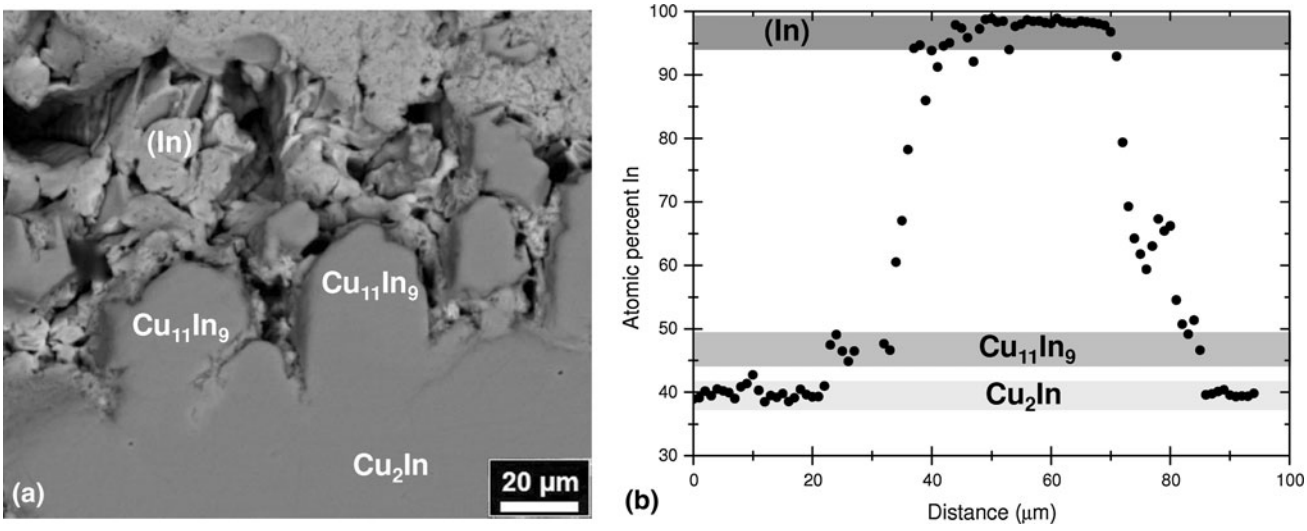

Fig. 2 (a) SEM image from sample I (45.0 at.% In). (b) Composition profile across sample I determined by WDS with a beam diameter of 1 μm

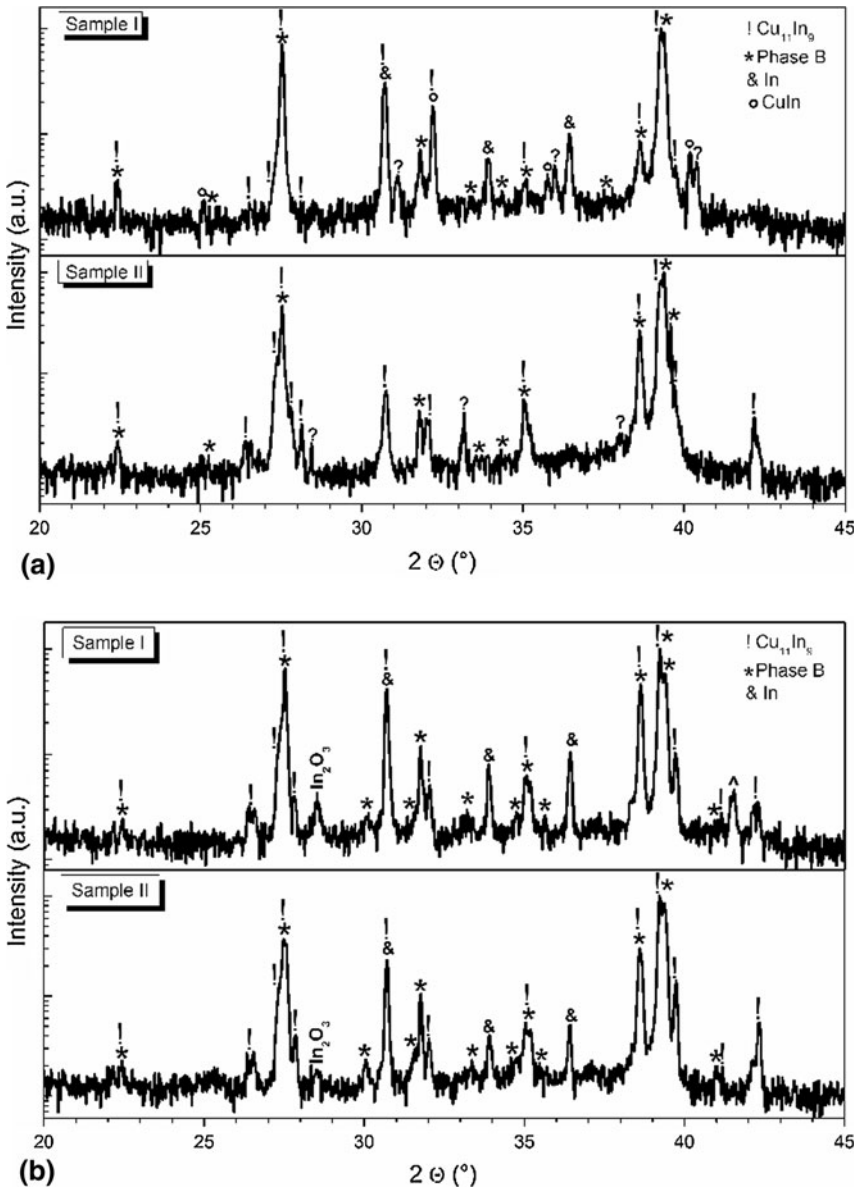

Fig. 3 S-PXRD patterns corresponding to samples I and II collected at room temperature (a) before and (b) after a thermal treatment up to 400 °C under Ar atmosphere. The intensity is in logarithmic scale. Peaks indicated as (?) were not identified. The peaks indicated as (^) correspond to the sample holder

In the diffraction pattern of sample I (Fig. 2a, above) collected at room temperature the presence of additional Bragg peaks corresponding to pure In[19] was clearly detected. This diffraction pattern also exhibits two peaks (i.e. 2Θ = 35.8° and 40.2°) that match the CuIn phase, a metastable phase that has been previously observed in Cu-In samples.[15,16]

Piao and Lidin[14] have recently reported a novel phase, $Cu_{10}In_7$, in a Cu-In alloy. The samples used by these authors were pre-heated at 820 °C for 24 h to get a homogeneous material, quenched in cold water and then subjected to a very long annealing (9 months) at 310 °C. According to these authors, this thermal treatment promoted the transformation from disordered $Cu_{11}In_9$ phase to a denser and ordered $Cu_{10}In_7$ compound. However, we have not detected in our x-ray patterns the presence of the Bragg peaks corresponding to this phase, even not in the sample with nominal composition $Cu_{10}In_7$ (41.2 at.% In). The absence of this novel phase in our samples is probably due to the fact that they were subjected to different homogenization procedures and annealed at a temperature slightly lower from those applied by Piao and Lidin.[14]

Figure 3(b) displays the S-PXRD patterns over 20-45° 2Θ angle for samples I and II, measured at room temperature after a thermal cycle of heating from 25 up to 400 °C and cooling back to 25 °C. The Bragg peaks

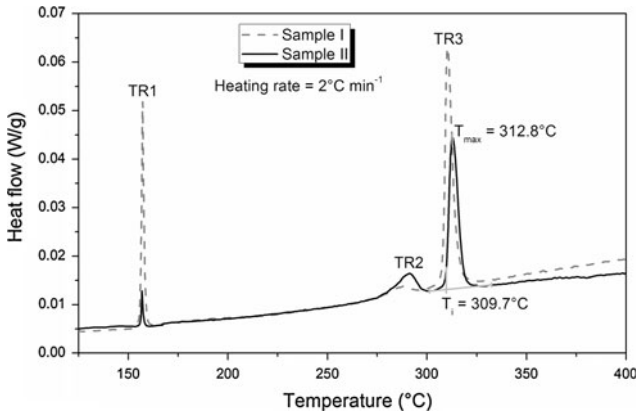

Fig. 4 DSC curves corresponding to samples I and II. T_i, T_{max} and the baseline are indicated for one selected peak

observed in the x-ray diffraction patterns displayed in Fig. 3(b) indicate that both alloys are mainly composed of three phases, namely $Cu_{11}In_9$,[17] B[11,12] and pure In.[19]

We can verify that all unidentified low intensity peaks detected in the diffraction patterns before the heating/cooling cycle (Fig. 3a) are absent in the patterns of the same samples after thermal cycling (Fig. 3b). Finally, we can notice in Fig. 3(b) that the Bragg peaks that matched those of the CuIn phase also disappeared after thermal cycling.

A weak Bragg peak at $2\Theta = 28.4°$ in Fig. 3(b) indicates the formation of a small amount of In_2O_3.[20] This oxide probably resulted from the presence of a small fraction of oxygen in the furnace during the heating/cooling cycle. The presence of this oxide may cause a slight shift in the sample composition towards the Cu-rich region and it could also stabilize other unexpected phases. The formation of indium oxide could also explain the disappearance of the CuIn metastable phase in sample I. Nevertheless, we consider that such a small amount of oxide does not affect the conclusions of the present work because the major phase present in the samples (i.e., $Cu_{11}In_9$) was formed during casting and/or annealing.

According to the Cu-In phase diagrams shown in Fig. 1(a) and (b),[8,9] in both studied samples below 310/307 °C, a pure In phase is not a priori expected. Thus, the results of our diffraction study suggest that the pure In phase detected at room temperature is not an equilibrium phase but a metastable phase retained from high temperature during the cooling process after casting and/or the annealing. Furthermore, as we can see in Fig. 1(a) and (b), the B phase is not expected to be present in sample I (45.0 at.% In). All these evidences indicate that samples I and II did not reach a full equilibrium state. This conclusion is a consequence of the known low inter-diffusion coefficients reported for the Cu-In system.[22,23]

3.2 DSC Analysis

The results of our DSC analysis of phase transitions in samples I and II are plotted in Fig. 4. Three transitions can be clearly observed: TR1, TR2, and TR3 at the temperatures reported in Table 2.

The first transition (TR1) begins at 156.1 and 156.3 °C for samples I and II, respectively. These temperatures are close to the melting temperature of pure In (i.e. 156.6 °C). Therefore, transition TR1 can be related to the melting of pure In present in the samples.

Transition TR2 starts at 277.2 °C for sample I and at 280.4 °C for sample II whereas TR3 initiates at 308.1 and 309.7 °C for samples I and II, respectively. These temperatures of the TR3 transition are in between those reported for the peritectic $\eta' + L \rightleftharpoons Cu_{11}In_9$ reaction by Bolcavage et al.[9] (i.e. 307 ± 1 °C) and by Subramanian and Laughlin[8] (i.e. 310 °C). In addition, no evidence of $A' \rightarrow A$ transition was detected in the DSC analysis, this transition being expected to occur at 350 °C according to the phase diagram plotted in Fig. 1(a). Accordingly, the results of the present DSC study are consistent with the existence of the $\eta + \eta°$ two-phase field proposed by Bolcavage et al.[9] in the 33-38 at.% In range. However, previous works[11,12] point out that this field at low temperature is composed of two phases (B and C).

3.3 Crystallographic Characterization at High Temperature

In-situ S-PXRD experiments were performed in order to identify the phases involved in the transitions observed by DSC technique.

Figure 5(a) shows the iso-intensity lines derived from the S-PXRD patterns on the 2Θ-T plane for sample I over the 27-31° 2Θ range, for temperatures ranging from 90 up to 375 °C. A similar result was obtained for sample II (not shown). Figure 5(b) displays the whole x-ray diffraction pattern recorded at the maximum temperature of the heating cycle (388 °C). The diffraction patterns displayed in Fig. 5(a) exhibit strong changes at 156 °C and within the 385-304 °C range at which phase transitions are expected to occur, according to DSC results.

Figure 6(a) displays the x-ray diffraction patterns recorded at temperatures close to the temperature of the first phase transition, labeled as TR1. We notice in Fig. 6(a) that the intensity of the Bragg peak at $2\Theta = 30.6°$ strongly decreases while the intensities of the other peaks remain nearly invariant. On the other hand, the Bragg peak corresponding to $2\Theta = 30.6°$ matches both the $Cu_{11}In_9$ phase and pure In. According to the phase diagrams of Fig. 1, the TR1 transition can be a priori assigned to either In melting at 156.6 °C or to the $L \rightleftharpoons Cu_{11}In_9 + (In)$ eutectic reaction at 153-154 °C. Notice that in the case of an eutectic reaction, the intensities of all Bragg peaks from $Cu_{11}In_9$ phase (located at 27.4, 27.5 and 27.8° 2Θ angles) would be expected to decrease. Since in Fig. 6(a) such trend was not observed for all Bragg peaks, the TR1 transition can safely be assigned to In melting.

A second transition (TR2) occurs in the 285-294 °C temperature range. Figure 6(b) displays x-ray diffraction patterns around this transition temperature. The intensity of the Bragg peak at $2\Theta = 30.6°$ (related to phase $Cu_{11}In_9$) exhibits a decrease at $T = 285$ °C and finally vanishes at

Table 2 Initial (T_i) and maximum (T_{max}) temperatures involved in the transitions characterized in the DSC curves displayed in Fig. 4

	TR1		TR2		TR3	
Sample	T_i (°C)	T_{max} (°C)	T_i (°C)	T_{max} (°C)	T_i (°C)	T_{max} (°C)
I	156.1	157.2	277.2	288.3	308.1	310.4
II	156.3	156.9	280.4	291.2	309.7	312.8

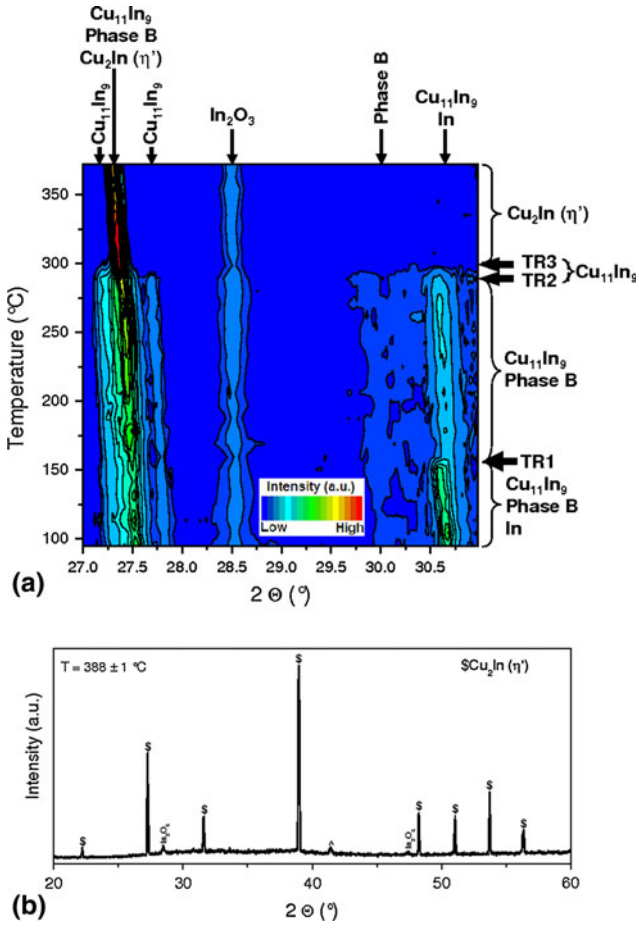

Fig. 5 (a) Temperature dependence of the in-situ x-ray diffraction patterns corresponding to sample I (45.0 at.% In). Peak positions corresponding to phases $Cu_{11}In_9$,[17] Cu_2In (η′),[13] B,[11,12] In[19] and In_2O_3[20] are also indicated. (b) Diffraction pattern recorded at the highest temperature (388 °C). The peaks indicated as (^) correspond to the sample holder

294 °C. At this temperature, the peaks at 27.7° and 29.9° (corresponding to the $Cu_{11}In_9$ and B phases, respectively) also disappear while the peak at 27.2° (related to phase $Cu_{11}In_9$) decreases noticeably (see also Fig. 5a). At the same time, the intensity of the peak at 27.4° (corresponding to both $Cu_{11}In_9$ and η′ phases) markedly increases. All this indicates that $Cu_{11}In_9$ and B phases transform to the high temperature η′ phase (Cu_2In),[13] according to the reaction $\eta' \rightleftharpoons B + Cu_{11}In_9$.[1]

A further increase in temperature to 304 °C produces the extinction of the peak at 27.2° (see Fig. 6c), which corresponds to phase $Cu_{11}In_9$. Above 304 °C and up to 388 °C only the peaks associated to the high temperature η′ phase remain (Fig. 5b). The relatively high and diffuse background observed within the $25° < 2\Theta < 45°$ range in the diffractogram of Fig. 5(b) is the expected effect produced by the melting of pure In melted during the TR1 transition. No evidence of the presence of A′ phase[7]—indicated in the phase diagrams displayed in Fig. 1(a)—was detected within the 304-388 °C temperature range. As a matter of fact, this phase would produce a strong Bragg peak at 2Θ close to 30° that is not present in the patterns shown in Figs. 5(a) and 6(c). Accordingly, the transition characterized from the x-ray diffraction patterns plotted in Fig. 6(c) can be related to the $\eta' + L \rightleftharpoons Cu_{11}In_9$ (TR3) transformation.

It is worth noticing that in the diffraction pattern recorded at 388 °C (Fig. 5b) the Bragg peaks corresponding to the A phase[11,12] were not detected. This phase, being a superstructure of the Cu_2In phase,[13] exhibits in its diffraction pattern additional low intensity peaks. On the other hand, phase A was detected in samples with a lower In content (over the 32-37 at.% In composition range) annealed during 7 months at 500 °C.[12] These findings could indicate that the 33-38 at.% In between 388 and 500 °C is composed of phases η′ and A at low and high temperatures, respectively; or, alternatively, that the features related to the superstructure of phase A appear during the cooling process.

4. Conclusions

The nature and thermal stability of phases in two Cu-In alloys with 45 and 41.2 at.% In nominal compositions, annealed at 300 °C for 7 months, were investigated over the 25-400 °C temperature range by means of the combined use of the SEM, WDS, S-PXRD and DSC techniques.

Our experimental results indicate that after quenching from 300 °C down to room temperature both samples are mainly composed of a $Cu_{11}In_9$ phase containing minor amounts of B phase and, in one of the studied samples (45.0 at.% In), also pure In metastably retained.

The presence of the $Cu_{10}In_7$ phase reported in a previous work[14] was not detected in our samples, not even in sample II, which has exactly the same nominal composition as the previously reported phase (Cu-41.2 at.% In). This

[1]Although this notation can be confusing since different nomenclatures are mixed, we use it to be consistent with the literature.

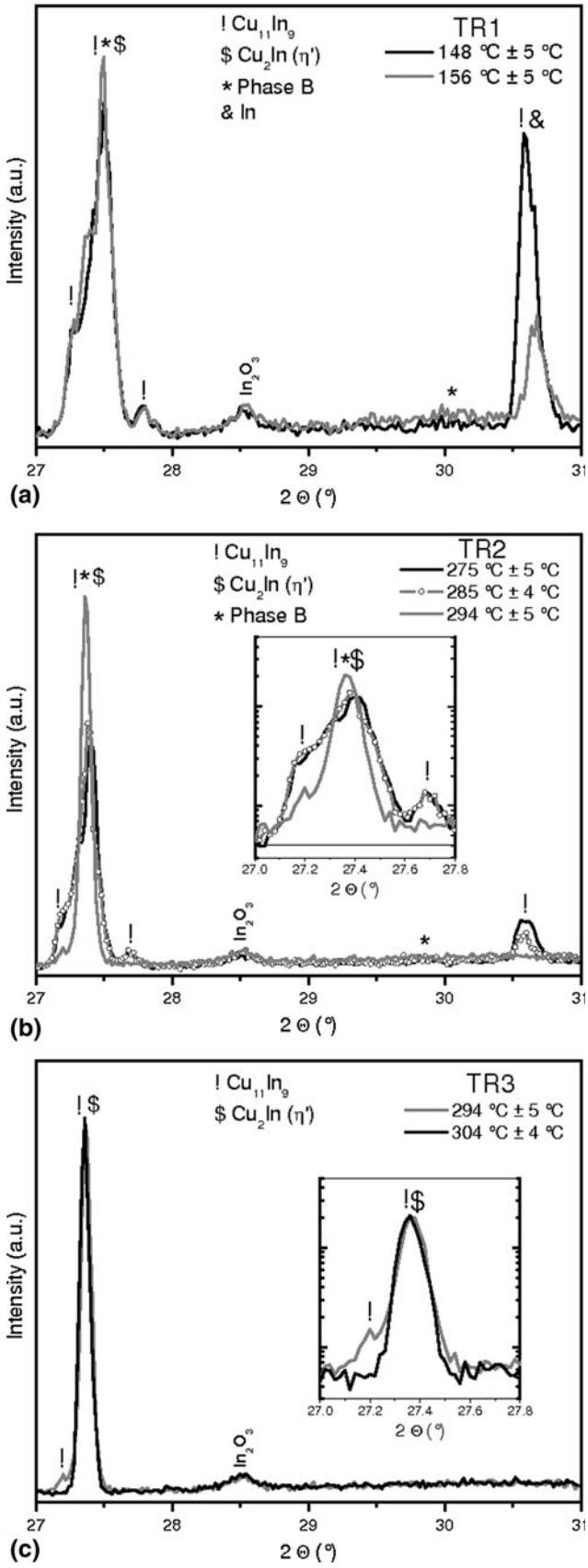

◀ **Fig. 6** Selected S-PXRD patterns corresponding to sample I (45.0 at.% In) recorded at different temperatures, close to the observed transition temperatures, (a) TR1, (b) TR2 and (c) TR3. The temperature uncertainty was taken as half the difference between maximum and minimum temperatures reached during the collection of each XPD pattern

probably occurred because the thermal conditions under which we have prepared this sample, namely a homogenization treatment during 7 months at 300 °C and even a further heating up to 400 °C at 2 °C/min, are not sufficient for promoting a noticeable formation of such phase.

Besides a low temperature phase transition at $T = 157$ °C related to the melting of residual In, two additional transitions were clearly identified: one of them at $T = 290$ °C corresponds to the $\eta' \rightleftharpoons B + Cu_{11}In_9$ reaction and a second one at $T = 311$ °C corresponding to a peritectic $\eta' + L \rightleftharpoons Cu_{11}In_9$ reaction. No evidence of any other phase transition over the 25-400 °C temperature range was detected.

Acknowledgments

This work was funded by FONCyT Project PICT 2006-1947, Comahue National University, CONICET, and LNLS (Brazil) under Research Proposal D10B-XPD-10810. The authors acknowledge the beamline staff at LNLS for technical assistance.

References

1. A.T. Dinsdale, A. Watson, A. Kroupa, J. Vrestal, A. Zemanova, and J. Vízdal, Eds., *COST Action 531-Atlas of Phase Diagrams for Lead-Free Soldering*, Vols 1 and 2, COST Office, Brussels, 2008
2. S.-W. Chen, C.-H. Wang, S.-K. Lin, and C.-N. Chiu, Phase Diagrams of Pb-Free Solders and Their Related Materials Systems, *J. Mater. Sci.: Mater. Electron.*, 2007, **18**, p 19-37
3. G. Zeng, S. Xue, L. Zhang, and L. Gao, Recent Advances on Sn-Cu Solders with Alloying Elements: Review, *J. Mater. Sci.: Mater. Electron.*, 2011, **22**, p 565-578
4. L. Yan, C. Lee, D. Yu, A. Yu, W.-K. Choi, J.-H. Lau, and S.-U. Yoon, A Hermetic Seal Using Composite Thin-Film In/Sn Solder as an Intermediate Layer and Its Interdiffusion Reaction with Cu, *J. Electron. Mater.*, 2009, **38**, p 200-207
5. S. Sommadossi and A. Fernández Guillermet, Interface Reaction Systematics in the Cu/In-48Sn/Cu System Bonded by Diffusion Soldering, *Intermetallics*, 2007, **15**, p 912-917
6. S. Sommadossi, W. Gust, and E.J. Mittemeijer, Characterization of the Reaction Process in Diffusion-Soldered Cu/In-48 at.% Sn/Cu Joints, *Mater. Chem. Phys.*, 2002, **77**, p 924-929
7. K.C. Jain, M. Ellner, and K. Schubert, Über die Phasen in der Nähe der Zusammensetzung $Cu_{64}In_{36}$ (On the Phases Occurring Near the Composition $Cu_{64}In_{36}$), *Z. Metallkd.*, 1972, **63**, p 456-461, in German
8. P.R. Subramanian and D.E. Laughlin, The Cu-In System, *Bull. Alloy Phase Diagr.*, 1989, **10**, p 554-610
9. A. Bolcavage, S.W. Chen, C.R. Kao, Y.A. Chang, and A.D. Romig, Jr., Phase Equilibria of the Cu-In System I: Experimental Investigation, *J. Phase Equilib.*, 1993, **14**, p 14-21

10. Z. Bahari, E. Dichi, B. Legendre, and J. Dugué, The Equilibrium Phase Diagram of the Copper-Indium System: A New Investigation, *Thermochim. Acta*, 2003, **401**, p 131-138
11. M. Elding-Pontén, L. Stenberg, and S. Lidin, The η-Phase Field of the Cu-In System, *J. Alloys Compd.*, 1997, **261**, p 162-171
12. L. Baqué, D. Torrado, G. Aurelio, D. Lamas, S. Aricó, A. Craievich, and S. Sommadossi, Crystallographic Characterization of Cu-In Alloys in the 30-37 at.% In Region, *Calphad*, 2013, **43**, p 1-6
13. G.C. Che and M. Ellner, Powder Crystal Data for the High-Temperature Phases Cu_4In, Cu_9In_4 (h) and Cu_2In (h), *Powder Diffr.*, 1992, **7**, p 107-108
14. S. Piao and S. Lidin, A New Compound in the Cu-In System—The Synthesis and Structure of $Cu_{10}In_7$, *Z. Anorg. Allg. Chem.*, 2008, **634**, p 2589-2593
15. V. Simic and Z. Marinkovic, Room Temperature Interactions in Copper-Metal Thin Film Couples, *J. Less-Common Met.*, 1980, **72**, p 133-140
16. J. Chang, J.H. Lee, J.-H. Cha, D.-Y. Jung, G. Choi, and G. Kim, Bimetallic Nanoparticles of Copper and Indium By Borohydride Reduction, *Thin Solid Films*, 2011, **519**, p 2176-2180
17. T.P. Rajasekharan and K. Schubert, Kristallstruktur von $Cu_{11}In_9$, *Z. Metallkd.*, 1981, **72**, p 275-278
18. S. Ramos de Debiaggi, G.F. Cabeza, C. Deluque Toro, A.M. Monti, S. Sommadossi, and A. Fernández Guillermet, Ab Initio Study of the Structural, Thermodynamic and Electronic Properties of the $Cu_{10}In_7$ Intermetallic Phase, *J. Alloys Compd.*, 2011, **509**, p 3238-3245
19. F. Swanson, *Natl. Bur. Stand. (U.S.)*, 1954, Circ. **539**, III, p 12
20. Swanson et al., *Natl. Bur. Stand. (U.S.)*, 1955, Circ. **539**, 5, p 26
21. Rodríguez-Carvajal, J., Recent Development of the Program FULLPROF, *Commission on Powder Diffraction (IUCr) Newsletter*, 2001, **26**, p 12-19
22. S. Sommadossi, W. Gust, and E.J. Mittemeijer, Phase Characterization and Kinectics Behavior of Diffusion Soldered Cu/In/Cu Interconnections, *Mater. Sci. Technol.*, 2003, **19**, p 528-534
23. D.-G. Kim, J.-W. Yoon, C.-Y. Lee, and S.-B. Jung, Reaction Diffusion and Formation of $Cu_{11}In_9$ and $In_{27}Ni_{10}$ Phases in the Couple of Indium-Substrates, *Mater. Trans.*, 2003, **44**, p 72-77